

Viscoelastic Properties of Amorphous Polymers. 6. Local Segmental Contribution to the Recoverable Compliance of Polymers

K. L. Ngai*

Naval Research Laboratory, Washington, D.C. 20375-5320

D. J. Plazek

Department of Materials Science and Engineering, University of Pittsburgh, Pittsburgh, Pennsylvania 15261

Isabel Echeverría

Física Fundamental, UNED, Apdo. 60141, 28080 Madrid, Spain

Received April 16, 1996; Revised Manuscript Received August 12, 1996[®]

ABSTRACT: A prominent shoulder exhibited in the shear retardation spectrum of a high molecular weight polystyrene enables the local segmental contribution to the recoverable compliance to be isolated and determined for the first time. The prominence of this shoulder depends on the time/frequency window of the viscoelastic measurements. This interesting dependence is explained by the thermorheological complexity of the glass–rubber softening dispersion.

Introduction

The identification of different modes of molecular motions in polymers and their contributions to the experimentally measured shear viscoelastic spectrum has always been the ultimate goal of most studies of polymer viscoelasticity.^{1,2} This task is not simple because of the long-chain nature of polymers. Modes of many different length scales will be involved. Moreover, because the chains are densely packed together in bulk polymer and concentrated solutions, intermolecular interactions will make some of the modes difficult to describe on a theoretical basis. Examples are the local segmental modes which are responsible for the onset of glassy behavior. The basic units of motion involve a few monomers, and the motions of the units are cooperative in nature due to the combination of intermolecular and intramolecular interactions. How exactly the cooperative motions of the units are to be described is currently still a frontier research problem. Furthermore, one would like to know what are the individual contributions that the local segmental motions and other modes (sub-Rouse^{2,3} and modified Rouse for undiluted polymers¹) of longer length scales make to the measured shear creep compliance $J(t)$ and the complex dynamic compliance $J^*(\omega)$ in the glass–rubber softening dispersion. In high molecular weight polymers, the creep compliance $J(t)$ increases from the glassy compliance $J_g \approx 10^{-10} \text{ cm}^2 \text{ dyn}^{-1}$ or 10^{-9} Pa^{-1} to the entanglement plateau compliance $J_N^\circ \approx 10^{-6} \text{ cm}^2 \text{ dyn}^{-1}$ or 10^{-5} Pa^{-1} as the glass–rubber softening dispersion is traversed.

In spite of the long history of research in viscoelasticity of polymers, the answers to the questions discussed above are still forthcoming. The main interest of the present work is the long-time limiting contribution of the local segmental motions, J_{ea} , to the recoverable compliance, $J_r(t) = J(t) - t/\eta$, where η is the zero-shear viscosity. The short-time limit of the local segmental contribution to the recoverable compliance is, by definition, the glassy compliance J_g . Although J_g

is well known and its magnitude can be readily obtained by experiment,^{1,4} no one has ever determined J_{ea} of a high molecular weight amorphous polymer. Recent combined experimental and theoretical studies of molecular motion in polymers have made some advances in identifying the different modes.^{1–3,5,6} Some conclusions obtained from mechanical compliance measurements are summarized in the next section. Donth and co-workers at the University of Halle, Halle, Germany, have helped in the same cause by performing dynamic mechanical modulus measurements and dual data analysis to obtain both the shear relaxation time spectrum $H(\log \tau)$ and the shear retardation time spectrum $L(\log \tau)$.^{7–9} With the assistance of dielectric and enthalpy relaxation measurements, Donth and co-workers (D) have identified the slight shoulder appearing at short τ 's in L , first found by Plazek and co-workers (P) in poly(vinyl acetate) (PVAc)¹⁰ and atactic polypropylene (a-PP),¹¹ to originate from local segmental modes which D refer to as the “proper glass transition”. Also, the location in time of the main peak in H is nearly the same as the slight shoulder in L .^{7–9} The shoulder being prominent in the L of PS and other high molecular weight polymers obtained by D allows the contribution from the local segmental mode, L_{α} , to be isolated. Integration over L_{α} gives us the long-time limiting contribution of the local segmental motions to the recoverable compliance, J_{ea} . We show below that the value of J_{ea} obtained in this manner for high molecular weight polystyrenes is in agreement with another method applicable only to low molecular weight polystyrenes and other polymers.^{2,12–15}

We will first present a summary of the important properties of the different modes in the glass–rubber softening transition which will be used later. This will be followed by a comparison of the creep and dynamic data. While a shoulder appears in the L of D,^{7–9} there is no trace of it in the L derived from the recoverable creep compliance of PS.¹⁶ The shoulder in L of D enables the isolation of the local segmental contribution to the recoverable compliance. The only difference between the two measurements is the time/frequency window.

[®] Abstract published in *Advance ACS Abstracts*, November 1, 1996.

Therefore, the prominence of the shoulder seems to depend on the time window of measurement. We shall explain this window effect by the properties of the viscoelastic modes and deduce the value of $J_{\text{e}\alpha}$ for PS and PVAc from the short-time shoulder of L .

Properties of Viscoelastic Modes in the Glass–Rubber Softening Dispersion

Although at this time we still do not have a full microscopic understanding of the viscoelastic modes in the glass–rubber softening region, some facts about the major viscoelastic modes have emerged^{2,3} from recent studies. Some of these deduced from experimental data² are summarized as follows.

(1) The local segmental motion (α -relaxation) additively contributes a compliance that is well approximated by the second term in eq 1^{2,13}

$$J_{\alpha}(t) = J_g + (J_{\text{e}\alpha} - J_g)[1 - \exp(-(t/\tau_{\alpha})^{1-n_{\alpha}})] \quad (1)$$

where $0 < 1 - n_{\alpha} \leq 1$ and the equilibrium compliance, $J_{\text{e}\alpha}$, has been determined only for low molecular weight polymers and is approximately

$$J_{\text{e}\alpha} \approx 4.0J_g \quad (2)$$

for polystyrene^{2,12} and

$$J_{\text{e}\alpha} \approx 5.0J_g \quad (2a)$$

for poly(methylphenylsiloxane).¹³ $J_g = 9 \times 10^{-10} \text{ Pa}^{-1}$ for PS and $5.4 \times 10^{-10} \text{ Pa}^{-1}$ for PMPS. These values of $J_{\text{e}\alpha}$ were deduced by taking advantage of the “encroachment” effect in low molecular weight polymers,^{12–14} which, at sufficiently low temperatures, entirely eliminates the polymeric mode contributions to the recoverable compliance to leave only the local segmental contributions (see Figures 50–52 of ref 2).

(2) The compliances, $J_R(t)$, contributed by the Rouse modes are higher than a lower cut-off, J_{Rc} , which was estimated^{2,17} to have the order of magnitude of 10^{-7} Pa^{-1} , although the exact size depends on the flexibility of the polymer through the minimum number of monomers required to make a Gaussian submolecule, the basic unit of a Rouse chain. For a high molecular weight polymer that has an entanglement plateau compliance J_N° , the bounds of $J_R(t)$ are given by

$$J_{\text{Rc}} \approx 10^{-7} \text{ Pa}^{-1} \leq J_R(t) \leq J_N^{\circ} \quad (3)$$

(3) The existence of polymeric (sub-Rouse) modes^{2,3,5,6} with length scales intermediate between the local segmental modes and the minimum wavelength of the Rouse modes has been established. The contribution, J_{SR} , from these sub-Rouse modes fills the compliance gap defined by eqs 1 and 3, i.e.,

$$J_{\text{e}\alpha} \leq J_{\text{SR}} \leq J_{\text{Rc}} \quad (4)$$

The total compliance in the glass–rubber softening dispersion is the sum

$$J(t) = J_{\alpha}(t) + J_{\text{SR}}(t) + J_R(t) \quad (5)$$

For most polymers, it is difficult to resolve the three groups of viscoelastic mechanism, α , sR, and R, in any of the viscoelastic functions because the glass–rubber dispersion is relatively narrow. However, in certain amorphous polymers like polyisobutylene (PIB), which

has a broader glass–rubber dispersion,^{1,18} they have been resolved^{2,3} by viscoelastic measurements made with different instruments to have a combined time window of nearly 10 decades.³

(4) The data showed that the shift factors, $a_{T,\alpha}$, $a_{T,\text{sR}}$ and $a_{T,R}$, of the α , sR, and R modes, respectively, in this order, have a decreasing temperature sensitivity.^{3,6} In other words, the retardation or relaxation times of the α mode shift by the largest amount, the sR mode by an intermediate amount, and the R modes by the least amount with an identical change in temperature. This experimental fact is consistent with what has been expected from the coupling parameter n_{α} of the coupling model. The model predicts^{13,18,19} that

$$a_{T,\alpha} = (a_{T,0})^{1/(1-n_{\alpha})} \quad (6)$$

and

$$a_{T,R} = a_{T,0} \quad (7)$$

where $a_{T,0}$ is the primitive shift factor in the coupling model and is the same for all modes. Most amorphous polymers have relatively large coupling parameters. For example, PS and PVAc have $n_{\alpha} = 0.64$ and 0.57 , respectively.^{20,21} On comparing eqs 6 and 7, we can conclude that the retardation/relaxation times of the α mode shifts with decreasing temperature to longer times faster than the R modes. Consequently, the separation between the α mode and the R modes decreases with decreasing temperature; i.e. the α mode encroaches the R modes of longer times. In Figure 1 we plot the shift factor of the softening dispersion, $a_{T,S}$, at temperatures near T_g (about 98°C) of a high molecular weight PS. At these low temperatures near T_g shown, the isothermal shear recoverable compliances measured are below 10^{-7} Pa^{-1} and are principally in the range of the local segmental modes defined by eq 1. Hence, $a_{T,S}$ should coincide with the shift factor specifically for the local segmental mode, $a_{T,\alpha}$, at these low temperatures. This expectation is confirmed by the good agreement of $a_{T,S}$, the shift factor of the softening dispersion obtained by creep compliance measurements,¹² with the temperature dependence of the α -relaxation times measured in the same temperature range by the 2D exchange NMR experiment²² that can monitor correlation times as long as $\sim 10^2 \text{ s}$. Using eqs 6 and 7 and $n_{\alpha} = 0.64$ for PS,^{20,21} we deduce the shift factors of the Rouse modes,

$$\log(a_{T,R}) = (1 - n_{\alpha}) \log(a_{T,\alpha}) \quad (8)$$

which have a weaker temperature dependence. Shown also in Figure 1 is the shift factor, $a_{T,\eta}$, of the viscosity, η . According to another prediction of the coupling model,^{18–21} the product $(1 - n_{\eta}) \log(a_{T,\eta})$ is also equal to $\log(a_{T,R})$, where $n_{\eta} \approx 0.41$. This product shown also in Figure 1 is in good agreement with $(1 - n_{\alpha})a_{T,\alpha}$.

The effects have been verified directly in PIB, where all the modes, α , sR, and R, were resolved from its broad mechanical spectrum^{2,3,13,18} and their shift factors determined in a common temperature range. Although $a_{T,\alpha}$ has a stronger temperature dependence than $a_{T,R}$ in PIB, the encroachment effect is comparatively weaker in PIB than in PVAc and PS because PIB has the smallest n_{α} among these three polymers (see also eqs 6 and 7). Incidentally, this is also the reason why PIB has a much broader softening dispersion than PVAc and PS.

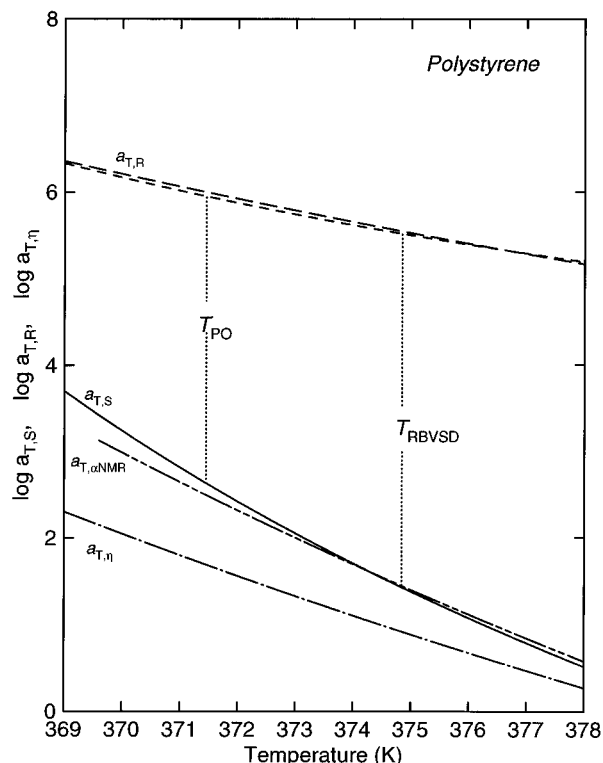


Figure 1. Shift factors, $a_{T,S}$ and $a_{T,\eta}$, of the softening dispersion and the terminal dispersion respectively of a high molecular weight polystyrene in a temperature range near T_g . In this limited temperature range, $a_{T,S}$ can be identified with the shift factor of the local segmental modes, $a_{T,\alpha}$, which is nearly the same as that, $a_{T,\alpha NMR}$, directly determined by NMR. All shift factors have been determined in the temperature range shown and no extrapolation has been used. Shown also are the products $(1 - n_\alpha) \log(a_{T,\alpha})$ and $(1 - n_\eta) \log(a_{T,\eta})$ (long-dashed and short-dashed curves, respectively). These products should be and are indeed equal, and both are identified with $\log(a_{T,R})$, the shift factors of the Rouse modes. PO, Plazek and O'Rourke;¹² RBVSD, Reissig et al.⁸ See discussion of T_{PO} and T_{RBVSD} in the text.

The order of temperature sensitivity, discussed above, should be noted to be contrary to all others observed in rate process transition maps.²³ The general rule is that shorter time mechanisms have smaller temperature sensitivities.

Determination of $J_{e\alpha}$

The various linear viscoelastic response functions, $G^*(\omega)$, $J^*(\omega)$, $G(t)$, and $J(t)$, and spectral distributions, $H(\tau)$ and $L(\tau)$, are related to each other by well-known exact relations.¹ Reissig, Beiner, Vieweg, Schröter, and Donth (RBVSD)⁸ measured dynamic shear modulus $G^*(\omega)$, and the master curve $G^*(a_{T,G}\omega)$ was constructed by time-temperature superpositioning the isothermal $G^*(\omega)$ experimental data. We use $a_{T,G}$ to denote the shift factors obtained by RBVSD. From $G^*(a_{T,G}\omega)$ they obtained the retardation spectra, $L(\tau/a_{T,G})$, by the exact relations between the viscoelastic functions by a numerical procedure called NLREG (nonlinear regularization).²⁴ Their result for polystyrene (PS)⁷⁻⁹ is shown as the dashed curve in Figure 2. The sample is a high molecular weight PS with $M_w = 706$ kg/mol. The terminal peak is not shown because the present interest is in the softening dispersion. As pointed out by RBVSD, a shoulder on the short-time portion of $L(\tau/a_{T,G})$ is apparent. With the assistance of dielectric and enthalpy relaxation measurements, Donth and co-workers (D)⁷⁻⁹ have concluded that the slight shoulder

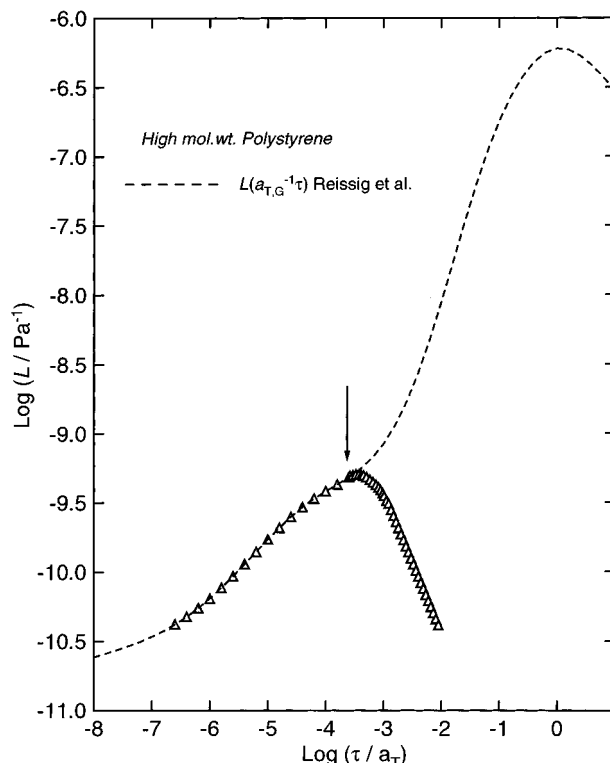


Figure 2. Shear retardation spectrum of a high molecular weight polystyrene (dashed curve) obtained by Reissig et al.⁷⁻⁹ Only the softening dispersion is shown. The peak defined by the triangles is isolated as the local segmental contribution in the manner described in the text. The vertical arrow indicates the point of inflection.

originates from the local segmental mode which is responsible for the glass transition. Also, the location in time of the main peak in H is nearly the same as that of the slight shoulder in L .⁷⁻⁹ The appearance of the short-time shoulder in the $L(\tau/a_{T,G})$ of RBVSD for polystyrene makes it possible to estimate the contribution, $L_\alpha(\tau/a_{T,G})$, of the local segmental mode. There is a point of inflection at some τ (its location suggested by the vertical arrow in Figure 2) indicating beyond which $L_\alpha(\tau/a_{T,G})$ will start to decrease. An estimate of the actual $L_\alpha(\tau/a_{T,G})$ is indicated by the small peak in Figure 2 which agrees with $L(\tau/a_{T,G})$ of RBVSD at short times and has a maximum value of $10^{-9.3}$ Pa⁻¹. The shape of $L_\alpha(\tau/a_{T,G})$ for times beyond the inflection point is somewhat arbitrary. Our construction is guided by the often-observed stretched exponential time dependence of the correlation function of local segmental modes observed by dielectric, photon correlation, and dynamic specific heat spectroscopies.⁷⁻⁹ For the compliance contributed by the local segmental mode, the stretched exponential dependence has been displayed in eq 1. $J_\alpha(t)$ calculated from the $L_\alpha(\tau/a_{T,G})$ shown in Figure 2 is well described by eq 1.

To ensure ourselves that the small $L_\alpha(\tau/a_{T,G})$ peak constructed in Figure 2 is an approximately correct representation of the local segmental mode, we compare it in Figure 3 with the retardation spectra, L_{3400} , of a low, 3400 molecular weight PS obtained numerically from the isothermal recoverable creep compliance measurement at three temperatures.¹² The data of L_{3400} (shown as open circles) were reduced to the reference temperature of 100.6 °C. An additional small shift of -0.2 decade is necessary to bring L_{3400} to coincide with $L(\tau/a_{T,G})$ of RBVSD (shown as the dashed curve) at short times. The proximity of the two L 's is due to the

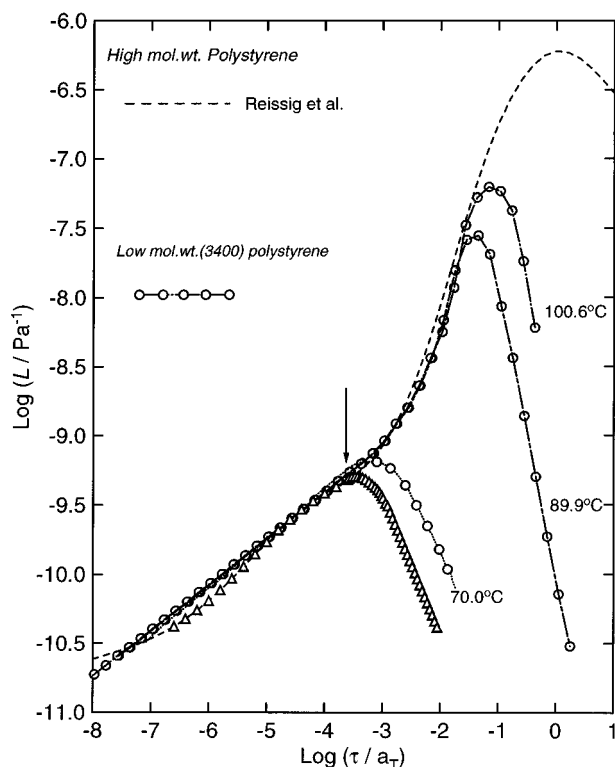


Figure 3. Shear retardation spectrum of the high molecular weight polystyrene of Reissig et al. (dashed curve) compared with the retardation spectra of a low (3.4 kg/mol) molecular weight polystyrene obtained at three temperatures (circles). As temperature is reduced, the polymeric modes are lost and at the lowest temperature of 70.0 °C, the retardation spectrum of the low molecular weight PS approaches the peak (triangles) of the high molecular weight PS in Figure 2.

choice of reference temperatures, which were both approximately 30 °C above T_g . As has been discussed elsewhere,^{2,12,14} the L of low molecular weight polymers PS exhibits the dramatic loss of contribution from polymeric modes as temperature is decreased toward T_g .¹² This interesting viscoelastic property is general because it occurs in other polymers, including poly(methylphenylsiloxane)¹³ and poly(propylene glycol).¹⁵ It has been explained also as a consequence of the local segmental modes encroaching the polymeric modes as T is lowered.¹⁴ At low molecular weights, large decreases in the peak of L are found which reflect the decrease in the steady-state recoverable compliance with decreasing temperatures near T_g .

$$J_e(T) = J_g + \int_{-\infty}^{\infty} L(\tau) d \ln \tau \quad (9)$$

Judging from the shape of L_{3400} at $T = 70.0$ °C, it is likely that at this temperature, L_{3400} arises almost solely from the contribution of the local segmental modes. The peak height of L_{3400} at 70.0 °C is $10^{-9.2}$ Pa⁻¹, which is about 26% larger than that of the $L_\alpha(\tau/a_{T,G})$ peak suggested for high molecular weight polystyrene in Figure 2. We conclude, from the approximate agreement with L_{3400} at 70.0 °C, the $L_\alpha(\tau/a_{T,G})$ peak in Figure 2 and reproduced in Figure 3 is a good estimate of the contribution from the local segmental mode in PS. Substituting $L_\alpha(\tau/a_{T,G})$ for L in eq 9, taking $J_g = 9 \times 10^{-10}$ Pa⁻¹, and evaluating the integral, we obtain $J_{e\alpha} \approx 3.5 \times 10^{-9}$ Pa⁻¹. As far as we know, this is the first determination of the local segmental contribution to the recoverable compliance of any high molecular weight polymer.

This value of $J_{e\alpha}$ obtained after isolating the $L_\alpha(\tau/a_{T,G})$ peak from the shoulder structure in RBVSD's data of high molecular weight PS is in good agreement with the value given by eq 2. The latter was read off directly from the long-time limiting recoverable compliance data of low molecular weight PS at temperatures near T_g .^{2,12} Such good agreement lends additional support to the interpretation of the short-time shoulder in $L_\alpha(\tau/a_{T,G})$ of high molecular weight polymers as the local segmental modes responsible for the onset of glassy behavior by Donth and co-workers and also by us.

Prominence of Shoulder: Dependence on the Experimental Time/Frequency Window

A comparison between the two sets of experimental data on high molecular weight polystyrene by RBVSD⁷⁻⁹ and by Plazek and O'Rourke (PO)¹² can be made in any one of the equivalent representations, $G^*(\omega)$, $J^*(\omega)$, $G(t)$, $J(t)$, $H(\tau)$, and $L(\tau)$. The data of PO and RBVSD are presented as the reduced curves $J(a_{T,J}t)$ and $G^*(a_{T,G}\omega)$, respectively. These were the result of the time-temperature reduction of isothermal $J(t)$ and $G^*(\omega)$ experimental data. We must be aware of the fact that actually time-temperature superposition of isothermal data in the softening dispersion does not work exactly for PS and PVAc^{10,11,25} as have been found by other workers²⁶⁻²⁸ and reconfirmed by the data of D.⁷⁻⁹ The failure of time-temperature superposition of the data of D can be seen most clearly in the loss tangent. The data cited that exhibit thermorheological complexity of the softening dispersion all indicate that the shift factor of the mechanisms contributing to the lower compliances (or lower L) has a more sensitive temperature dependence than that of mechanisms contributing at longer times and larger compliances. This behavior of the shift factors is in accord with property (4) given above where the modes of molecular motion contributing to the softening dispersion are broken down into three principal types as described in paragraphs (1)–(3) of the last section. Nevertheless, compromised master curves, $J(a_{T,J}t)$ and $G^*(a_{T,G}\omega)$, of the data were obtained. Their retardation spectra of high molecular weight polystyrene, $L(a_{T,J}\tau)$ of PO and $L(\tau/a_{T,G})$ of RBVSD, obtained by numerical procedures from the respective reduced curves are shown in Figure 4. Only data of $\log(L/\text{Pa}^{-1}) \leq -9$ are shown in this figure because our present interest is the local segmental modes which are located in this region of the softening transition. In constructing Figure 4, $L(a_{T,J}\tau)$ of PO (solid curve) was shifted to shorter reduced times such that the rising contribution to L , above the local segmental contribution $L_\alpha(\tau/a_{T,G})$ and due to the sub-Rouse modes, occur at the same position as $L(\tau/a_{T,G})$ of RBVSD (dashed curve). The horizontal shift is necessary because the reference temperature, T_0 , of time-temperature superposition chosen by PO is 100 °C, which is much lower than 129 °C employed by RBVSD. After lining up the upper parts of the two L 's in Figure 4, a difference between the two sets of data in the vicinity of the local segmental modes becomes apparent. While the short-time shoulder is prominent in the $L(\tau/a_{T,G})$ of RBVSD, it disappears in the $L(a_{T,J}\tau)$ of PO. Moreover, the short-time portion of $L(a_{T,J}\tau)$ that is less than $10^{-9.3}$ Pa⁻¹ appears at longer times than the corresponding portion of $L(a_{T,G}^{-1}\tau)$ by 0.39 decade. The entire $L_\alpha(\tau/a_{T,G})$, defined by the peak structure (triangles), when shifted to longer times by the same amount gives rise to another peak (circles) in Figure 4. The latter would be the corresponding local

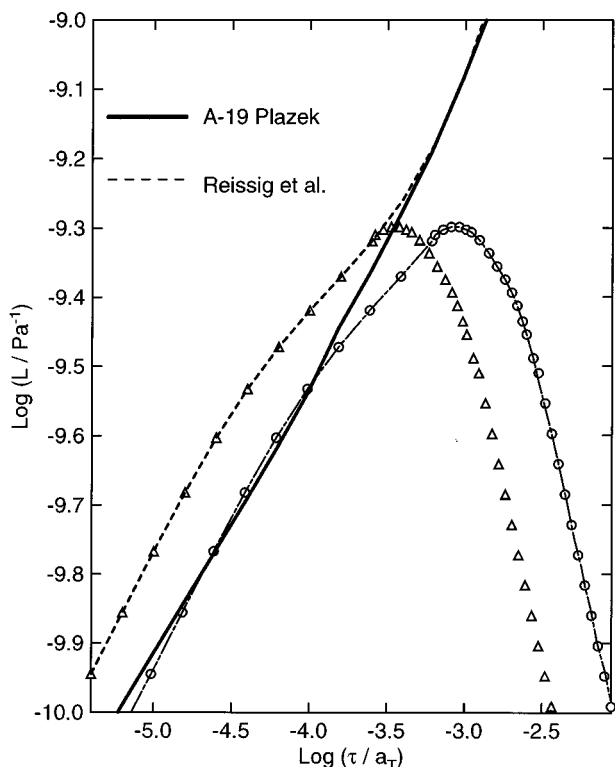


Figure 4. Comparison of the retardation spectra of PS obtained by Plazek and O'Rourke (solid curve) with Reissig et al. (dashed curve) in the vicinity of the local segmental contribution. The peak (circles) is obtained from the local segmental contribution extracted from the data of Reissig et al. (triangles) by a horizontal shift of 0.39 decade.

segmental contribution, $L_\alpha(a_{T,j}\tau)$, to the $L(a_{T,j}\tau)$ of PO. In fact, the circles overlap the data of PO for $L(a_{T,j}\tau) < 10^{-9.5} \text{ Pa}^{-1}$ rather well. Thus, the disappearance of the shoulder in the $L(a_{T,j}\tau)$ of PO seems to be caused by the shift of $L_\alpha(a_{T,j}\tau)$ by 0.39 decade to longer times and getting buried under the rapidly rising contributions of the sub-Rouse modes.

The data of RBVSD were taken in the frequency range 0.01–100 rad/s, which corresponds to a factor of about 100 times shorter than the time window of creep compliance measurement of P. Therefore, the prominence of the shoulder as well as the width of the softening dispersion depends on the time/frequency window of measurement. This trend can be explained by the stronger temperature dependence of $a_{T,\alpha}$ compared with the shift factors, $a_{T,sR}$ and $a_{T,R}$, of the polymeric modes. Measurements by an instrument that has a longer time/lower frequency window are made at lower temperatures. Consequently, the separation in time scales of the local segmental mode and the polymeric modes becomes smaller, because the time scale of the former has encroached further toward the latter. In Figure 1 we have placed the two shift factors $a_{T,\alpha}$ and $a_{T,R}$ relative to each other such that their separation roughly corresponds to the distance (about 4 decades) between the positions of the peak and the short-time shoulder in the $L(\tau/a_{T,G})$ data of RBVSD. There, we indicate by the two vertical dotted lines the lowest temperatures of observation, T_{PO} and T_{RBVSD} , reached in the measurements of PO and RBVSD, respectively, at which the most probable retardation time or relaxation frequency of the local segmental mode still lies within the experimental window. In going from RBVSD's measurement to PO's measurement, the length of the dotted line becomes shorter. The difference in

the lengths of the two dotted lines is 0.7 decade. We expect that this difference has the same order of magnitude as the separation of the short-time portions of $L(\tau/a_{T,G})$ and $L(a_{T,j}\tau)$ shown in Figure 4, where, by construction, the retardation times of the sub-Rouse (not the Rouse modes) modes in the vicinity of the local segmental modes are the same for both measurements. As we have shown, the separation between the two L 's is 0.39 decade, and this expectation is indeed the case. Therefore, the difference in the prominence of the shoulder between the two sets of data taken in two different experimental time windows (Figure 4) is caused by the local segmental modes encroaching the polymeric modes. The effect of encroachment is stronger at lower measurement temperatures reached in using creep compliance instruments which have a longer time window. This is in agreement with what is predicted from eqs 6–8 and illustrated in Figure 1.

Conclusion

Although one of us (D.J.P.) and co-workers found a slight shoulder in the shear retardation spectra of PVAc and polypropylene obtained from recoverable creep compliance measurement, not much physical significance had been attached to it. Moreover, the shoulder was not evident in the retardation spectrum of polystyrene. Therefore it was not sure whether this is a real effect or caused by experimental errors or time-temperature reduction of the data. Recently, RBVSD^{7–9} have made extensive shear dynamic modulus measurements and confirmed the presence of the shoulder in their retardation spectra in several polymers including PVAc and polystyrene. The shoulder is sufficiently prominent in the retardation spectrum of polystyrene of RBVSD to permit the contribution of the local segmental motion, L_α , to be isolated for the first time in any high molecular weight amorphous polymer. This result for L_α is confirmed by the retardation spectra of a low molecular weight polystyrene using the "encroachment effect". The latter removes nearly all the polymeric mode contributions to the viscoelastic response as temperature is decreased down to the glass temperature, leaving only the local segmental contribution. The long-time limit of the recoverable compliance contributed by the local segmental modes, J_{ea} , has been determined to have the value of $3.5 \times 10^{-9} \text{ Pa}^{-1}$ for high molecular weight polystyrene.

We have investigated the reason why the shoulder appears prominently in the retardation spectrum of polystyrene of RBVSD but disappears in the data of PO. The origin of this phenomenon lies in the thermorheological complexity of the softening dispersion, with the shift factor of local segmental modes having the most sensitive temperature dependence. The experimental time window of the creep compliance measurement of PO extends to longer times than the dynamic modulus measurement of RBVSD. As a consequence, measurement of the viscoelastic response of local segmental modes was carried out by PO to lower temperatures than by RBVSD and the separation in time scales of the local segmental modes and the polymeric sub-Rouse modes becomes smaller in PO's measurement, resulting in the disappearance of the shoulder.

The results of this work have enhanced our understanding of the properties of the various modes contributing to the viscoelastic response of the softening dispersion of high molecular weight polymers.

Acknowledgment. K.L.N. is supported in part by ONR Contract N0001496WX20267. The authors wish to thank S. Reissig, M. Beiner, S. Vieweg, K. Schröter, and E. Donth for making their dynamic modulus measurement available, which makes the detailed comparison with our shear recoverable compliance data possible.

References and Notes

- (1) Ferry, J. D. *Viscoelastic Properties of Polymers*, 3rd ed.; Wiley: New York, 1980.
- (2) Ngai, K. L.; Plazek, D. J. *Rubber Chem. Technol. Rubber Rev.* **1995**, *68*, 376.
- (3) Plazek, D. J.; Chay, I. C.; Ngai, K. L.; Roland, C. M. *Macromolecules* **1995**, *28*, 6432.
- (4) Plazek, D. J. *J. Non-Cryst. Solids* **1991**, *131–133*, 836.
- (5) Santangelo, P.; Ngai, K. L.; Roland, C. M. *Macromolecules* **1993**, *26*, 2682.
- (6) Rizo, A. K.; Jian, T.; Ngai, K. L. *Macromolecules* **1995**, *28*, 517.
- (7) Reissig, S.; Beiner, M.; Korus, J.; Schröter, K.; Donth, E. *Macromolecules* **1995**, *28*, 5394.
- (8) Reissig, S.; Beiner, M.; Vieweg, S.; Schröter, K.; Donth, E. *Macromolecules*, in press.
- (9) Donth, E.; Beiner, M.; Reissig, S.; Korus, J.; Garwe, F.; Vieweg, S.; Kahle, S.; Hempel, E.; Schröter, K. *Macromolecules*, in press.
- (10) Plazek, D. J. *Polym. J.* **1980**, *12*, 43.
- (11) Plazek, D. L.; Plazek, D. J. *Macromolecules* **1983**, *16*, 1469.
- (12) Plazek, D. J.; O'Rourke, V. M. *J. Polym. Sci., Part A-2* **1971**, *9*, 209.
- (13) Plazek, D. J.; Bero, C.; Neumeister, S.; Floudas, G.; Fytas, G. *Colloid Polym. Sci.* **1994**, *272*, 1430.
- (14) Ngai, K. L.; Plazek, D. J.; Bero, C. *Macromolecules* **1993**, *26*, 1065.
- (15) Cochrane, J.; Harrison, G.; Lamb, J.; Phillips, D. W. *Polymer* **1980**, *21*, 837. Ngai, K. L.; Schönhals, A.; Schlosser, E. *Macromolecules* **1992**, *25*, 4519.
- (16) Berry, G. C.; Plazek, D. J. in *Glass Science and Technology*; Uhlmann, D. R., Kreidl, N. J., Eds.; Academic: New York, 1996; Vol. 3, p 363.
- (17) Williams, M. L. *J. Polym. Sci.* **1962**, *62*, 57.
- (18) Plazek, D. J.; Zheng, X. D.; Ngai, K. L. *Macromolecules* **1992**, *25*, 4920.
- (19) Ngai, K. L. *Disorder Effects on Relaxational Processes*; Richert, R., Blumen, A., Eds.; Springer-Verlag: Berlin, 1994; p 89.
- (20) Plazek, D. J.; Ngai, K. L. *Macromolecules* **1991**, *24*, 1222.
- (21) Ngai, K. L.; Plazek, D. J. *J. Polym. Sci., Part B: Polym. Phys.* **1986**, *24*, 619.
- (22) Spiess, H. W. *J. Non-Cryst. Solids* **1991**, *131–133*, 766. Kaufmann, S.; Wefing, S.; Schaefer, D.; Spiess, H. W. *J. Chem. Phys.* **1990**, *93*, 197.
- (23) McCrum, N. G.; Read, B. E.; Williams, G. *Anelastic and Dielectric Effects in Polymeric Solids*; Wiley: London, 1967.
- (24) Honerkamp, J.; Weese, J. *Rheol. Acta* **1993**, *32*, 63.
- (25) Plazek, D. J. *J. Polym. Sci. Part A-2* **1968**, *6*, 621.
- (26) Cavaille, J.-Y.; Jordan, C.; Perez, J.; Monnerie, L.; Johari, G. *J. Polym. Sci., Part B* **1987**, *25*, 1235.
- (27) Connolly, R., unpublished data. See Figures 41c and 41d in ref 2.
- (28) Palade, L. I.; Verney, V.; Attené, P. *Macromolecules* **1995**, *28*, 7051.

MA9605558